

CYCLIC ACCELERATION TECHNIQUE FOR SOLVING UNSTEADY TRANSONIC SMALL PERTURBATION EQUATIONS

I Wayan Tjatra , Irvan Wandana

Aerodynamics Laboratory , Inter University Center for Engineering Sciences
Institut Teknologi Bandung
Jl. Ganesha 10 , Bandung 40132 , Indonesia

Abstract

An efficient cyclic acceleration scheme was developed base upon implicit approximate factorization (AF) algorithm for the solution of unsteady transonic flow problems. The presence of shock waves in the flow fields and its interactions with boundary layer , in general , will degrade the performance of an AF scheme. Therefore, this algorithm has to be accelerated in order to reduced the iteration number at each time-step. An acceleration coefficient , α , with cyclic values was added into the right-hand side (residual part) of the ξ sweep during the Newton iteration process in the original scheme. It was shown that the use of cyclic α values improved convergence rate of the original scheme. Computations were made on NACA0012 airfoil with sinusoidal movement for several combination values of free-stream Mach number , movement amplitude and reduced frequencies . Numerical results were , then , compared with available.

Introduction

The main difficulty in transonic flow computation is that the flow structure is complex and inherently nonlinear which is typified by the appearance of shock-waves in the flows. The complexity of this flow structure becomes more pronounced because of the fact that (as indicated in the wind tunnel experiments) the shock waves are also moving. The shocks oscillate forward and backward following the aeroelastic movement of the body surface¹.

In general , transonic flows should be mathematically described by nonlinear equations of mixed elliptic/hyperbolic type , since the subsonic flow is described by elliptic equation and supersonic flow by hyperbolic one. Boundary between solutions of these two equations (the shock waves) must be found as part of the solution. If self the difficulty is that analytic solutions of these mixed equations are generally not available. Therefore, it is more convenience to solve these nonlinear transonic flow equations numerically. There are many numerical methods available for predicting characteristic of steady and unsteady transonic flows. The complexity of equations that need to be solved depends on the characteristics of the flow and (for aeroelastic analysis) the coupling mechanism between the aerodynamic and structural model (of the moving surface) used in the analysis. Perhaps the most complex flow is the one induced by structure oscillating at large amplitude with strong shock waves motion, such that the flow is separated. To incorporate the whole complexities of this

kind of flow structure , there are little alternative other than to use and solve the Navier - Stoke's equations. The simplest equations that can describe a typical transonic flow is the linearized transonic small disturbance (TSD) equations .

Murman and Cole² developed the first computer program for the solution of unsteady transonic small disturbance equations based on SLOR shock capturing finite difference algorithm. It was shown in ref. 2 , that this solution procedure is more efficient computationally than the explicit , time-accurate procedure proposed by Magnus and Yoshihara for Euler equations. Although this procedure proven to be accurate and reliable, its routine application is limited only for certain problems because of low convergence-rate characteristic of the scheme. This approximation is valid for reduced frequency of the body surface oscillation less than 0.2 which add another restriction for aeroelastic applications (flutter can be found at reduced frequency as high as 0.5).

At present , methods based on the small disturbance theory have already led to the development of computer code that are in routine use for aeroelastic applications , such as ATRAN3S and CAP-TSD (code developed at NASA Langley) . ATRAN3S , the NASA Ames version of XTRAN3S , is a three-dimensional code based on a time-accurate , finite difference method using alternating direction implicit (ADI) algorithm. Several terms of the TSD equation in the ADI algorithm used in this code are treated explicitly , which leads to a time step restriction based on numerical stability consideration. It was shown that the number of time steps required per

cycle increases with a decrease in the aspect ratio and taper ratio and an increase in the sweep angle, movement amplitude and reduced frequency of the moving structure³. Code based on ADI algorithm, like this one, becomes very expensive for three-dimensional applications not just because of the small time-step needed in obtaining a convergence results, but also because of the fact that all of the sweep in the algorithm can be written in vectorized form. An approximate factorization (AF) algorithm developed by Batina³, that is applied in CAP-TSD, was proven more efficient for three-dimensional flow calculations. This AF algorithm consists of a time-linearization procedure (to determine estimate values of the perturbation potential) coupled with a Newton iteration technique (to provide time accuracy in the solutions). Newton iteration process occupied most of the cpu time needed for stable and accurate results.

The main objective of this work is to developed a stable new procedure based on the AF algorithm with higher efficiency and accuracy. From previous studies, it was found that the Newton iteration technique employed in the original AF algorithm was a major source of slow convergency. Therefore, a modified iteration sweep was developed. This new iteration making use an acceleration coefficient α in the ξ -sweep which given a cyclic values. The addition of this coefficient gives stable and accurate results with less iteration number per time step. With the modified procedure, unsteady flow computations are made for several combination values of free-stream Mach number, movement amplitude and reduced frequencies and comparison are made with the available data.

Approximate Factorization Algorithm

In this study, the transonic flows is governed by the modified transonic small disturbance (TSD) equations which may be written in conservation law form as

$$\frac{\partial f_0}{\partial t} + \frac{\partial f_1}{\partial x} + \frac{\partial f_2}{\partial z} = 0 \quad [1]$$

$$f_0 = -B\phi_{,x} + A\phi_{,t} \quad f_1 = E\phi_{,x} + F\phi^2_{,x} \quad f_2 = \phi_{,z}$$

where t is the non-dimensional time = $k\bar{t}$

k is the reduced frequency of the movement, and

ϕ is the disturbance potential velocity

Coefficients A , B and E are defined as

$$A = M^2 k^2, \quad B = 2M^2 k, \quad E = 1 - M^2$$

in which M represents the free-stream Mach number.

There are several choices for coefficients F being used, depending upon the assumptions made in deriving TSD equation. In this study, this coefficient is defined as

$$F = -\frac{1}{2} [3 - (2-\gamma)M^2] M^2$$

Boundary conditions imposed upon the flow field are those of non-reflecting boundary defined by Kwak⁴, as

$$\text{Far upstream} : \quad \phi = 0 \quad [2.a]$$

$$\text{Far downstream} : \quad \frac{1}{2} \left[\frac{-B}{C} + \frac{D}{\sqrt{C}} \right] \phi_{,t} + \phi_{,x} = 0 \quad [2.b]$$

$$\text{Far above and below} : \quad \frac{1}{2} D \phi_{,t} + \phi_{,z} = 0 \quad [2.c]$$

The surface flow tangency boundary condition is written in the form

$$\phi_{,z}^{\pm} = f_{,x}^{\pm} + f_{,t}^{\pm} \quad [2.d]$$

and imposed at the mean plane of the oscillating surface.

For unsteady flow calculations based on TSD equation, surface boundary conditions need not to be applied on the actual body surface. Instead, it is applied on the mean surface of the body. Therefore, a body-fitted grid system is not required. Numerical computations are carried out in a computational domain within a rectangular region conform to the airfoil which is obtained by a coordinate transformation of the physical domain. The physical grid system in (x, z) plane is transformed into some (ξ, ζ) plane, so that the mesh spacing in both directions can be kept uniform in the computational plane a using a trigonometric transformation function as defined in ref. 5.

An approximate factorization (AF) algorithm developed by Batina⁶, is used in this investigations. This AF algorithm consists of a time linearization step to determine an estimate values of the perturbation potential coupled with a Newton iteration step to provide time accuracy in the solution, as shown in figure 1 below.

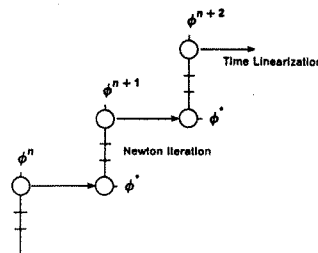


Figure 1. Approximate Factorization scheme for unsteady flow calculations

The mathematical formulations of this AF algorithm are derived using second-order accurate finite difference formulae in time and space, which may be presented as

$$L_{\xi} L_{\zeta} (\Delta\phi) = R(\phi^*, \phi^n, \phi^{n-1}, \phi^{n-2}) \quad [4]$$

$$L_{\xi} = 1 + \left(\frac{3B}{4A} \right) \xi_x \Delta t \frac{\partial}{\partial \xi} - \xi_x \left(\frac{\Delta t^2}{2A} \right) \frac{\partial}{\partial \zeta} F_1 \frac{\partial}{\partial \zeta}$$

$$L_{\zeta} = 1 - \left(\frac{\Delta t^2}{2A} \right) \frac{\partial}{\partial \zeta} F_3 \frac{\partial}{\partial \zeta}$$

Detail derivation of this equation can be found in ref. 5 . Equation [4] is solved through two - sweeps in the computational domain by sequentially applying the differential operators as

$$\xi - \text{sweep} : L_{\xi} \Delta \phi = -\omega R (\varphi^*, \varphi^n, \varphi^{n-1}, \varphi^{n-2}) \quad [5.a]$$

$$\zeta - \text{sweep} : L_{\zeta} \Delta \phi = \Delta \phi \quad [5.b]$$

In the first sweep, the calculation is carried out along grid-lines in the streamwise direction. Using the intermediate value $\Delta \phi$, the second sweep is performed along the vertical grid-lines to obtained $\Delta \phi$ values at each grid-points. With the updated values of $\Delta \phi$, the new values of the perturbation potential are obtained from

$$\varphi^{n+1} = \varphi^* + \Delta \phi \quad [6]$$

For each time step , computation is started with an estimate values of φ^* and is carried out until a convergence solution for φ^{n+1} is obtained (until the perturbation error in $\Delta \phi$ reaches the value of 10^{-6}). Using the φ^{n+1} values , the time linearization step is carried through to obtained the new estimate value φ^* for the next time-step. In this step, the airfoil is put at its new position (so , an updated surface boundary conditions are applied). The unsteady solutions are initiated using the steady-state solution as the first estimate values.

In most of the computation that had been performed using the original AF scheme , a minimum of 5 and maximum of 11 Newton iterations for each time-step are needed to obtained converged solution. For 360 time-steps per cycle, a total of maximum 3960 iterations required which use most of the total cpu time in the calculation. Although , in general , this scheme does not have a time step restriction , decreasing the number of time-step per cycle in order to reduce the total number of Newton iterations is not recommended since it will decrease the accuracy of the solutions. Another way that can be used for reducing the iteration number is by making use of an acceleration coefficient , α .

Cyclic Acceleration

A cyclic acceleration coefficient , α , which contains Δt , the time step , is added into the right hand side (residual R) during the ξ - sweep , so that equation [5.a] become

$$L_{\xi} \Delta \phi = -\alpha \omega R (\varphi^*, \varphi^n, \varphi^{n-1}, \varphi^{n-2}) \quad [7]$$

In the present study, the values of α is given a variation according to a geometric sequence defined by

$$\alpha_k = \alpha_{\max} \left(\frac{\alpha_{\min}}{\alpha_{\max}} \right)^{(k-1)/(k_n-1)} \quad [8]$$

where $k = 1, 2, 3, \dots, k_n$ with k_n represent the number of α_k values to be defined (usually between 4 to 8) . The α_{\max} and α_{\min} parameters represent the maximum and minimum values of α , respectively , which are defined as

$$\alpha_{\max} = 1 \quad , \quad \alpha_{\min} = \frac{4}{(\Delta z)^2} \quad [9]$$

For each Newton iteration , a different value of acceleration coefficient is used according to equation [8]. From the computation made using this modified AF scheme, it was found that stability and convergence rate of the solutions strongly depends on the variation of α values being used (the value of k_n). In this study , several values of k_n were chosen (according to the problem being treated) in order to optimize the number of Newton iteration required for convergence results.

Computed Results

The accuracy of the present method is evaluated by selecting several test cases recommended by AGARD⁷ , and comparing the computed results with the available measured data. Only cases for NACA0012 are presented in this report with test condition given in Table 1 . The reduced frequency , k , is calculated based on the semichord length.

Motions of the airfoil are described by the following harmonic equations :

$$\text{pitching motion} : \alpha(t) = \alpha_m + \alpha_0 \sin \Omega t$$

$$\text{plunging motion} : h(t) = h_0 \sin \Omega t$$

In these equations , α_m is the mean angle of attack, and Ω is the non-dimensional motion frequency (= $2kU/c$). In all cases, three or four cycles of unsteady motion are calculated in order to allow transients response to decay and using steady flow potential as a starting potential

distribution. Each cycle, in general, is divided into 360 time-steps. A linearized formula given in ref. 6 is used for the calculation of pressure coefficients.

For each cases, computational result are presented in the form of : upper and lower surface pressure distribution, lift and moment coefficient, and the real and imaginary parts of the first harmonic component of the pressure computed from the Fourier transform of the normalized (by the motion amplitude) aerodynamic response.

All numerical computation are obtained for the values of $\omega = 0.9$ and maximum and minimum cyclic acceleration coefficients given by equation [9]. For a maximum error in the disturbance potential equal to 10^{-6} , a maximum of three Newton iterations per time step are needed (compare to eleven for the calculations using no acceleration coefficient).

The four cases studied for NACA0012 airfoil listed in Table 1 involve greater mean angle of attack, $\alpha_m = 4.86$ degree, and larger pitching amplitude, $\alpha_0 = 4.59$ degree. Figure 2 presents the steady pressure distributions for the analytical and experimental cases at Mach number, $M = 0.950$ and $\alpha_m = 0$ degree. The shock strength and position at the upper surface of the inviscid solution is nearly coincide with the experimental data. A lower degree of agreement in shock strength and position found for a larger value of mean angle of attack. The convergence rate of this calculation given in Figure 3. A convergent result was obtained in just after 20 iterations. Meanwhile, similar results calculated using scheme without acceleration need at least 80 iterations.

Case	M	N_{Re}	α_m (deg)	α_0 (deg)	k
1	0.599	4.8×10^6	3.16	4.59	0.081
2	0.599	4.8×10^6	4.86	2.44	0.081
3	0.601	4.8×10^6	2.89	2.41	0.081
4	0.755	5.5×10^6	0.02	2.51	0.081

Table 1. NACA0012 airfoil test cases

In Figure 4, the upper and lower surface pressure distribution are plotted at free stream Mach number, $M = 0.599$, $\alpha_m = 4.86$ degree, $\alpha_0 = 2.44$ degree and reduced frequency of the airfoil motion equal to 0.081. Comparison with measurement data at several time-steps shows good agreement except for the shock strength and position close to the leading edge. Inviscid pressure distribution in present study has a stronger shock with an aftward position. This phenomena is always encountered in the inviscid potential flow solutions at high angle of attack due to the singularity of the leading-edge which affecting the upper surface solution. Similar results are obtained also for airfoil oscillate at a larger pitching amplitude, as shown in Figure 5. The maximum upper surface pressure at the airfoil leading-edge is lower than its experimental value. At this pitching motion

amplitude, the inviscid solution can not predict shock strength and position properly which indicate the limitation of small disturbance theory. The use of smaller grid size at the shock position could not reduce this singularity effects entirely. A leading-edge modification procedure proposed by Grossman and Melnik, as described in ref. 8, might be able to improve the accuracy close to the leading edge. In both cases, however, the lower surface pressure distributions are in very good agreement with experimental results.

Variation of the lift and moment coefficients with angle of attack for airfoil oscillatory cases 1 and 2 are presented in Figure 6. The shape of both plots are similar to that given in ref. 9 with a slightly different values.

Calculations at slightly higher freestream Mach number but at lower motion amplitude, case 3, shows a better leading edge pressure distribution. The pressure jump is lower compared to the previous result. But the shock strength and position is still not accurately predicted.

For cases at higher Mach number, calculations are performed at lower motion amplitude to ensure the validity of small-disturbance theory. Figure 7 presents the unsteady pressure distributions on the upper surface of the airfoil for NACA0012 case number 4 at freestream Mach number, $M = 0.755$. Comparison are made with the experimental data at every half-cycle of the motion after the completion of 3 full oscillation cycles. As with the previous results, the predicted shock location is slightly forward of the experimental location with a weaker jump in pressure distribution. Downstream of the shock, the analytic prediction agree fairly well with the experiment. Not as in the case with a large motion amplitude, there is no leading edge singularity effects found. Pressure distribution in the leading edge area are smoothly defined which are also in very good agreement with the experimental results. The variation of the lift and moment coefficients for a full one oscillation cycle are presented by close curves as shown in Figure 8. These close curves indicate that there are no transient aerodynamic response involve.

Conclusions

This paper has presented a study of cyclic acceleration technique for the unsteady two-dimensional transonic flow solutions. An acceleration coefficient with cyclic values is introduced in an approximate factorization (AF) scheme to solve the transonic small disturbance equations in order to accelerate the scheme convergence. The computer code with this acceleration coefficient included yields the number of Newton iteration needed for convergent results that are reduced by a factor of 5 from those based on the original scheme. Comparisons of unsteady pressure distribution and forces with the experimental results for transonic flow around NACA0012 airfoil shows a fairly good agreement.

Discrepancies of the results are mainly due to the singularity effects of the leading edge (due to large oscillation amplitude) and viscosity effects. Further investigations is required to include the leading edge modification and viscosity - shock interactions.

Acknowledgment

This work is partially supported by the National Research Council (DRN) through RUT II projects.

References

1. Tijdeman, H. , "Investigation of the transonic flow around oscillating airfoils" , National Aerospace Laboratory, NLR TR 77090U , The Netherland , 1978.
2. Murman, E. and J.D. Cole , "Calculation of plane steady transonic flows" , AIAA Journal , vol. 9 , no. 2 , February 1971.

3. Batina, J.T. , "An efficient algorithm for solution of the unsteady transonic small disturbance equation" , NASA TM 89014 , December 1986.
4. Kwak, D. , "Non-reflecting farfield boundary conditions for unsteady transonic flow computation" , AIAA Paper 80-1393 , 1980
5. Tjatra, I.W. , R.K. Kapania and B. Grossman , "Transonic flutter analysis of aerodynamic surfaces in the presence of structural nonlinearities" , Computing System in Engineering , vol. 1 , no. 2 , 1990.
6. Batina, J.T. , et.al. , "Unsteady transonic flow calculation for realistic aircraft configurations" , AIAA Paper 87-0850 , April 1987.
7. Bland, S.R., compiler , "AGARD two-dimensional aeroelastic configurations" , AGARD AR - 156 , Aug. 1979.
8. Melnik, R.E., "Turbulent interactions on airfoil at transonic speeds - recent developments" , AGARD CP - 291 , Feb. 1981.
9. Howlet, J.T. and Bland, S.R., "Calculation of viscous effects on transonic oscillating airfoils and comparisons with experiment" , NASA TP - 2731 , Sep. 1987.

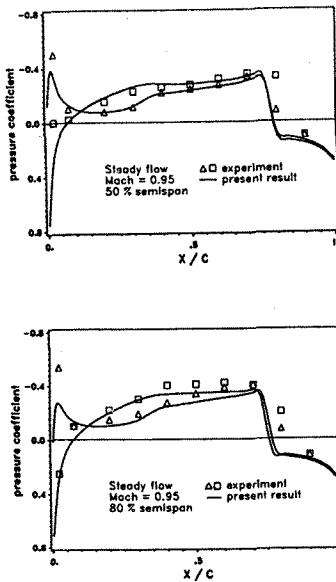


Figure 2. Steady pressure distribution of NACA0012 airfoil at $M = 0.950$ and $\alpha_m = 0$ deg.

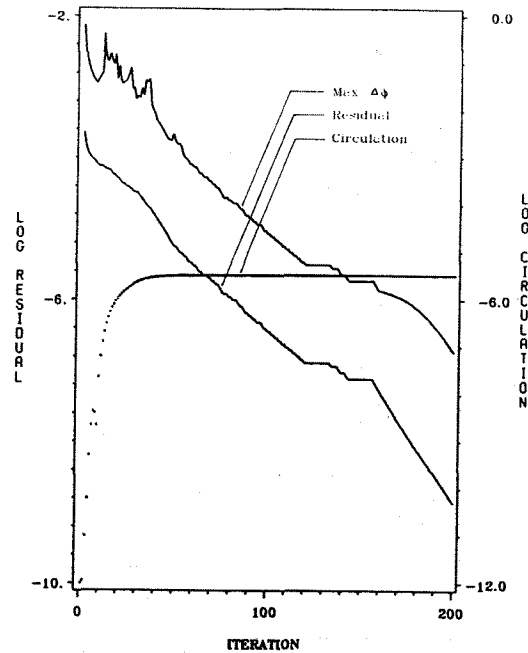


Figure 3. Convergence rate of flow calculations around NACA0012 airfoil

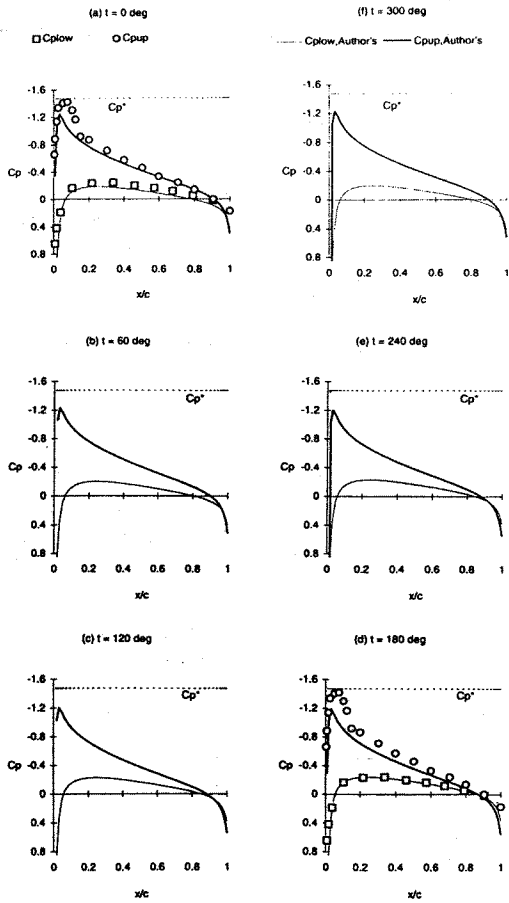


Figure 4. Unsteady pressure distribution of NACA0012 airfoil at $M = 0.599$, $\alpha_m = 4.86$ deg., $\alpha_0 = 2.44$ deg., and $k = 0.081$

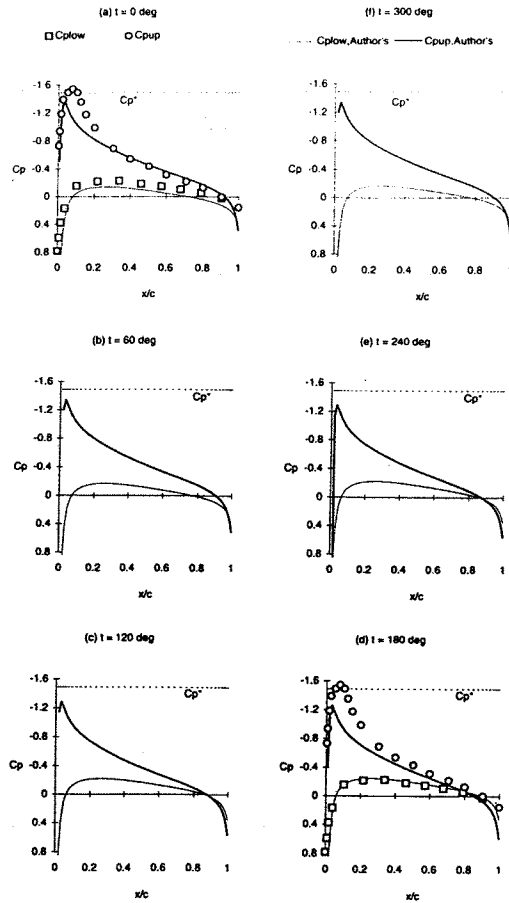


Figure 5. Unsteady pressure distribution of NACA0012 airfoil at $M = 0.599$, $\alpha_m = 3.16$ deg., $\alpha_0 = 4.59$ deg., and $k = 0.081$

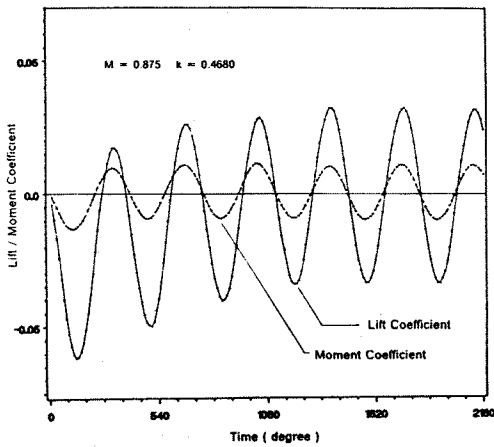


Figure 6. Variation of C_l and C_m coefficients with α for one full oscillation cycle at $M = 0.599$, $\alpha_m = 4.86$ deg. and $\alpha_0 = 2.44$ deg.

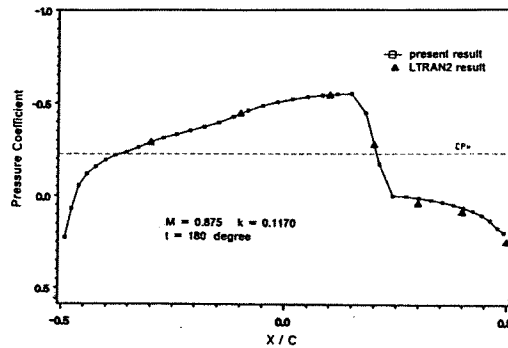


Figure 7. Unsteady pressure distribution of NACA0012 airfoil at $M = 0.755$, $\alpha_m = 0.02$ deg., $\alpha_0 = 2.51$ deg., and $k = 0.081$.

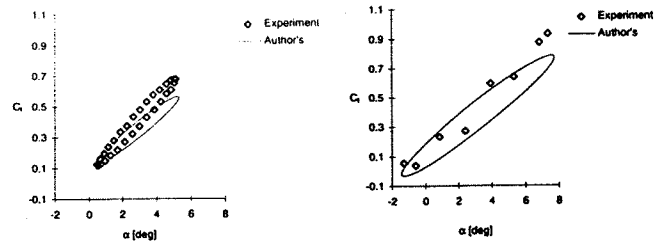


Figure 8. Variation of C_l and C_m coefficients with α for one full oscillation cycle at $M = 0.755$, $\alpha_m = 0.02$ deg. and $\alpha_0 = 2.51$ deg.